Electrocatalysis

International Edition: DOI: 10.1002/anie.201501590
German Edition: DOI: 10.1002/ange.201501590

Designing a Highly Active Metal-Free Oxygen Reduction Catalyst in Membrane Electrode Assemblies for Alkaline Fuel Cells: Effects of Pore Size and Doping-Site Position**

*Seonggyu Lee, Myounghoon Choun, Youngjin Ye, Jaeyoung Lee, Yeongdong Mun, Eunae Kang, Jongkook Hwang, Young-Ho Lee, Chae-Ho Shin, Seung-Hyeon Moon, Soo-Kil Kim, Eunsung Lee, and Jinwoo Lee**

Abstract: *To promote the oxygen reduction reaction of metal-free catalysts, the introduction of porous structure is considered as a desirable approach because the structure can enhance mass transport and host many catalytic active sites. However, most of the previous studies reported only half-cell characterization; therefore, studies on membrane electrode assembly (MEA) are still insufficient. Furthermore, the effect of doping-site position in the structure has not been investigated. Here, we report the synthesis of highly active metal-free catalysts in MEAs by controlling pore size and doping-site position. Both influence the accessibility of reactants to doping sites, which affects utilization of doping sites and mass-transport properties. Finally, an N,P-codoped ordered mesoporous carbon with a large pore size and precisely controlled doping-site position showed a remarkable on-set potential and produced 70% of the maximum power density obtained using Pt/C.*

Low-temperature fuel cells have been developed as next-generation energy sources. However, this technology is limited by a sluggish oxygen reduction reaction (ORR), which requires scarce and expensive catalysts such as Pt. To overcome these drawbacks, inexpensive and efficient ORR catalysts must be developed. In this regard, alkaline anion exchange membrane fuel cells (AEMFCs) have attracted attention because the ORR is more facile in an alkaline environment and therefore may facilitate the use of less expensive catalysts.[1] In AEMFCs, use of metal-free ORR catalysts based on heteroatom-doped carbon materials is a promising approach to replace Pt catalysts. Doping carbon with heteroatoms such as nitrogen, boron, and phosphorus enhances the ORR activity significantly compared with that in pure carbon. Theoretical and empirical evidences suggest that this enhancement occurs because the incorporation of heteroatoms changes the charge and spin density of carbon.[2] Recently, it has been shown that doping of multiple heteroatoms into the carbon structure further enhances the activity.[3]

For practical applications, research on the MEA is very important because it directly determines the performance of fuel cells. In MEAs, mass transport of reactants and products in the catalyst layer has a critical influence on cell performance, in addition to ORR activity. For example, the thick catalyst layer severely hinders mass transport and leads to poor cell performance. However, a relatively thick catalyst layer is required in metal-free catalysts compared with Pt catalysts because of their relatively low volumetric mass density and ORR activity. Thus, it is important to enhance mass transport in the catalyst layer, along with the improvement in ORR.

Porous carbon-based materials with ordered structure are promising candidates for highly efficient metal-free catalysts in MEAs because the porous structure enhances mass transport and provides many catalytically active sites.[4] Several studies on ordered porous metal-free catalysts have been reported using a hard template and a colloidal templating method.[5] However, the previous studies have only considered half cells, although the effect of mass transport is minimized in half cells due to the reduced diffusion length using a thin-film rotating disk electrode (RDE) technique.[6]

[*] S. Lee, Y. Ye, Y. Mun, Dr. E. Kang, J. Hwang, Prof. Dr. J. Lee
Department of Chemical Engineering
Pohang University of Science and Technology (POSTECH)
Pohang 790-784 (Republic of Korea)
E-mail: jinwoo03@postech.ac.kr
M. Choun, Prof. Dr. J. Lee, Prof. Dr. S.-H. Moon
School of Environmental Science and Engineering
Gwangu Institute of Science and Technology
Gwangju 500-712 (Republic of Korea)
Y.-H. Lee, Prof. Dr. C.-H. Shin
Department of Chemical Engineering
Chungbuk National University
Cheongju 360-763 (Republic of Korea)
Prof. Dr. S.-K. Kim
School of Integrative Engineering, Chung-Ang University
Seoul 156-756 (Republic of Korea)
Prof. Dr. E. Lee
Department of Chemistry
Pohang University of Science and Technology (POSTECH)
Pohang 790-784 (Republic of Korea)

[**] This work was supported by the National Research Foundation of Korea (NRF) grant funded by the Korea government (MSIP) (no. 2012R1A2A2A01002879 and 2013R1A1A2074550). This work was further supported by a grant of the Korea Health 21 R&D Project of Ministry of Health & Welfare (A121631), and by a grant from the Korea CCS R&D Center (KCRC) funded by the Korea government (NRF-2014M1A8A1049349).

Supporting information for this article is available on the WWW under http://dx.doi.org/10.1002/anie.201501590.

To fully utilize active sites in porous structured catalysts, precise control of the position of catalytically active sites is important. For example, in zeolite catalysts, full utilization of catalytically active sites on the micropores is often impossible because of low accessibility, even though the reactants are smaller than the micropores.[7] In contrast, active sites located on mesopores showed higher accessibility than those on micropores.[8] Therefore, better utilization of doping sites and enhancement of mass transport are expected in metal-free catalysts when most of the doping sites are located at the surface of large pores. However, the effect of doping-site position in a porous structure has never been studied.

From this point of view, it is necessary to properly determine the effect of pore size and doping-site position in MEAs based on metal-free catalysts, along with optimization of the catalytic activity for oxygen reduction in half-cell characterization. To the best of our knowledge, a systematic study on the effect of pore size and doping-site positions on the single-cell performance of metal-free catalysts has never been reported, although information from such studies would be helpful to guide the design of metal-free catalysts.

Herein, we report a strategy to construct highly active metal-free catalysts in MEAs by introducing a porous structure with controlled position of doping sites. The synthesized N,P-codoped ordered mesoporous carbon catalysts with large pores showed outstanding ORR activities and had superior methanol tolerance and durability compared with Pt/C in a half-cell test. Furthermore, the synthesized catalyst with precisely controlled doping-site position on the surface of large mesopores achieved a remarkable on-set potential compared with previously reported metal-free catalysts, and produced 70% of the maximum power density obtained by Pt/C in AEMFCs.

We used simple block-copolymer-assisted evaporation-induced self-assembly (EISA; Figure 1a) to prepare phosphorus-doped ordered mesoporous carbon (POMC) with large pores. EISA is a simple and efficient way to achieve well-connected large pores with high surface area, and allows functional materials to be directly incorporated into the structures during the self-assembly process.[9] We used an amphiphilic diblock copolymer, polystyrene-*b*-poly(ethylene oxide) (PS-*b*-PEO) as a structure-directing agent, resol as a carbon precursor, silicate oligomer (from hydrolysis of tetraethylorthosilicate) as a silica precursor, and hydrophobic tri(*p*-tolyl)phosphine (TPTP) as a phosphorus doping precursor. EISA yielded an ordered two-dimensional (2D) hexagonal structure because of the microphase separation caused by the different affinities of precursors to the parts of the block copolymer.

The hydrophilic resol and silicate oligomers mixed with hydrophilic PEO block by hydrogen bonding to form the framework of the mesostructure; the hydrophobic TPTP co-assembled with hydrophobic PS block to form confined cylindrical domains. Subsequent carbonization at 850°C converted the frameworks (hydrophilic domain) to walls composed of carbon–silica composite, and converted the cylindrical (PS-TPTP) domains to mesopores enclosed by phosphorus-doped carbon surfaces. The confinement of TPTP within the PS domain enables the formation of

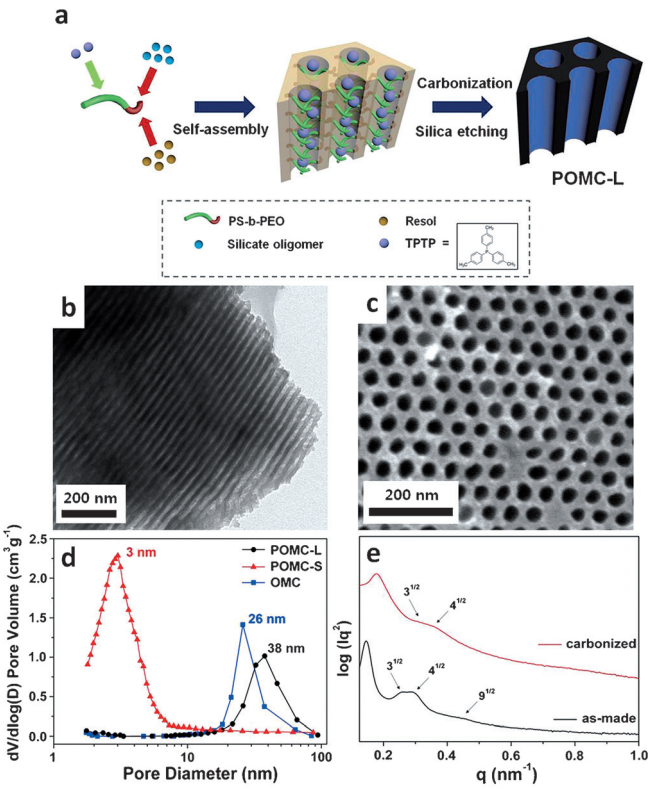

Figure 1. a) Representation of the synthesis of POMC-L. b) TEM and c) SEM image of POMC-L. d) Barrett–Joyner–Halenda (BJH) pore size distribution curves of POMC-L, POMC-S, and OMC. e) SAXS patterns of as-made and carbonized POMC-L.

phosphorus doping on the surfaces of the mesopores. Finally, etching to remove silica yielded the POMC with large pores (POMC-L). For comparison, we fabricated two additional samples: 1) to isolate the effect of the phosphorus doping, we used the same method without TPTP to synthesize a phosphorus-free ordered mesoporous carbon (OMC) with large pores; and 2) to isolate the effect of pore size, we used a previously reported hard-template method[5b] to prepare a POMC with small pores (POMC-S).

POMC-L, POMC-S, and OMC had well-defined ordered mesoporous structure, confirmed by transmission electron microscopy (TEM) and scanning electron microscopy (SEM) (Figure 1b,c and Figure S1 in the Supporting Information). The pore structure of the samples was also investigated using nitrogen physisorption. All samples had high surface areas of 1020–1110 $m^2 g^{-1}$ within 10% variance (Figure S2, Table S1). Pore size distribution curves calculated using the BJH method showed that the pore size was 38 nm in POMC-L, 26 nm in OMC, and 3 nm in POMC-S (Figure 1d). The difference in the pore sizes of POMC-L and OMC is interesting because they were synthesized using the same block copolymer; the only difference in their syntheses was the use of TPTP, and thus the selective interaction between hydrophobic TPTP and PS caused the pore expansion in POMC-L.

The uniformity of the porous structure in long-range order was confirmed using a small-angle X-ray scattering (SAXS) measurement. In the SAXS pattern of as-made POMC-L, the

peak positions of the relative scattering vector q occurred at $3^{1/2}$, $4^{1/2}$, and $9^{1/2}$ of the first-order maximum (Figure 1e). This result indicates that as-made POMC-L exhibits a long-range 2D hexagonally ordered mesoporous structure. The scattering pattern after carbonization showed a peak position ratio of $1:3^{1/2}:4^{1/2}$; therefore carbonized POMC-L maintained the highly ordered structure. The q values of all peaks become larger because of shrinkage of the framework during carbonization. The amount and chemical bonding state of phosphorus were investigated using X-ray photoelectron spectroscopy (XPS; Figure S3). The phosphorus to carbon ratio (P/C) was 0.43 atomic percent (at.%) in POMC-L and 1.03 at.% in POMC-S. P–C bonding (132 eV) in a high-resolution P 2p XPS spectrum revealed that phosphorus atoms were well-incorporated into the carbon matrix.[2e]

To test the ORR activities of the catalysts, linear sweep voltammetry (LSV) with RDE was conducted in a typical three-electrode cell. The LSV polarization curves (Figure 2a) showed that OMC without phosphorus doping had an on-set potential at 0.81 V and a half-wave potential at 0.69 V. Both POMCs showed positively shifted on-set and half-wave potentials, compared with OMC; these results confirm that the phosphorus doping accelerates the ORR by modifying the electronic structure of carbon. POMC-S has slightly better activity than POMC-L in terms of a half-wave potential.

Single-cell tests were conducted to investigate the effect of pore size. Cell performances of the MEAs differed greatly depending on whether POMC-L or POMC-S was used as the cathode catalyst. The maximum power density of POMC-L was 69 mW cm^{-2}, which is 3.5-fold higher than that of POMC-S (Figure 2b). At low current density, the voltage shows a linear relationship with log value of current density (Figure S4), so called Tafel behavior; this trend indicates that the reaction is kinetically controlled in this region. Activation loss of POMC-L and POMC-S was almost the same in the low current density region; this similarity means that the two POMCs have similar kinetic activity. However, the polarization curve of POMC-S drastically decreased as the current density increased, because the small pores of POMC-S impede mass transport, whereas the large pores of POMC-L enable efficient diffusion of reactants and products. Furthermore, POMC-L provides easier access to doping sites than does POMC-S because some of the doping sites in POMC-S are embedded in the walls of catalysts (Figure S5). Thus, precise control of the position of doping sites in mesoporous metal-free catalysts can be expected to enhance single-cell performance.

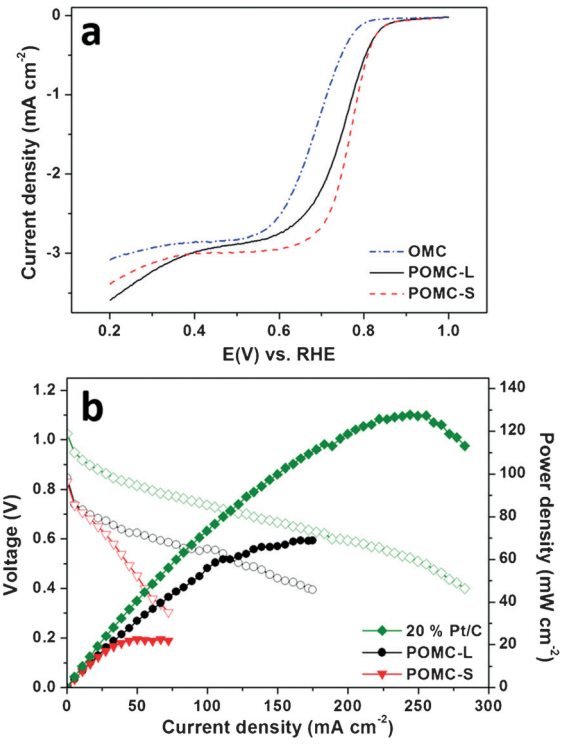

Figure 2. a) LSV polarization curves of the catalysts. b) Polarization curves of MEAs at 60 °C; open and closed symbols correspond to cell voltage and power density, respectively.

Although this study of POMC-L and POMC-S has demonstrated that pore size and position of doping sites are critical to improve single-cell performance, the maximum power density of POMC-L was only about 50% that of Pt/C. Therefore, we introduced additional nitrogen doping (Figure 3) to POMC-L to further enhance the catalytic

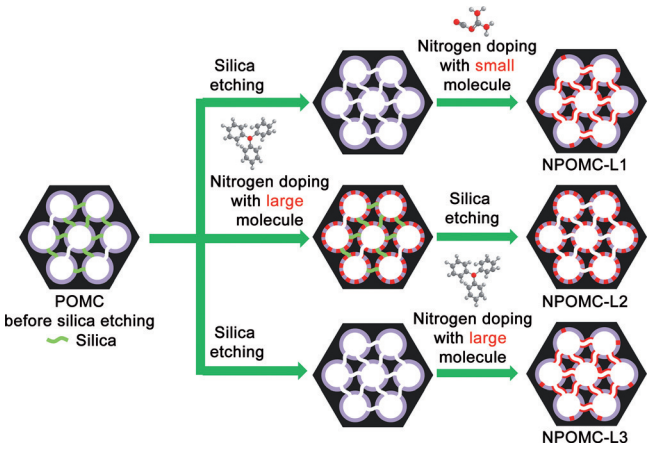

Figure 3. Representation of the synthetic conditions for additional nitrogen doping.

ORR activity. Two different conditions were used to show the effect of the position of doping sites. In condition 1, nitrogen was doped to POMC-L using a small molecule, dicyandiamide (DCDA), after etching to remove silica that had been used to maintain the structure during carbonization. DCDA molecules are smaller than the micropores in the carbons, which were obtained by etching of silica and carbonization of resol (Figure S6). Thus, the nitrogen-doping sites would form principally in the microporous region rather than in the mesoporous region of the resulting material (NPOMC-L1). In condition 2, nitrogen was doped to POMC-L using a larger molecule, triphenylamine (TPA), before silica etching. TPA molecules are larger than the micropores generated during carbonization of resol (Figure S6), and thus the doping sites would be mainly located in

the mesoporous region of the resulting material (NPOMC-L2).

The ordered structure was still maintained in both NPOMC-L1 and NPOMC-L2 after the additional nitrogen doping, confirmed by SEM, TEM, and nitrogen physisorption experiments (Figure S7). XPS analysis was performed to investigate the amount and chemical bonding state of nitrogen (Figure S8). The nitrogen contents obtained by XPS were assessed as 1.28 at.% in NPOMC-L1 and 0.82 at.% in NPOMC-L2, which are in good agreement with those obtained by CHN elemental analysis (1.30 at.% in NPOMC-L1 and 0.89 at.% in NPOMC-L2). The high-resolution N 1s spectrum of each sample was deconvoluted into four different nitrogen species, which correspond to pyridinic-N (398.2 eV, N1), pyrrolic-N (399.5 eV, N2), graphitic-N (401.2 eV, N3), and pyridinic-N^+-O^- (403.0 eV, N4).[5c] The deconvolution results of both samples show similar trends in the proportions of each nitrogen species (Table S2). Both NPOMCs were mostly composed of graphitic-N and pyridinic-N, which have been reported as the most highly active sites for ORR among these four nitrogen species.[2c,d]

The LSV polarization curves (Figure 4a) showed that the additional nitrogen doping significantly improved the kinetic activity to a level comparable to that of Pt/C. NPOMC-L1 exhibited an on-set potential at 0.95 V and a half-wave potential at 0.82 V, which are among the best activities reported for metal-free ORR catalysts.[2c,3b,c] All LSV curves measured in O_2-saturated solution in this work were corrected by subtracting the capacitive current measured in Ar-saturated solution.[10] Without the correction, the activity of carbon-based metal-free catalysts is often overestimated owing to their high capacitance (Figure S9). NPOMC-L1 also showed superb kinetic current density at 0.80 V (7.97 mA cm^{-2}). NPOMC-L2 exhibited an on-set potential at 0.92 V and a half-wave potential at 0.82 V, which are also remarkable activities but slightly lower than NPOMC-L1. The Tafel slopes of both NPOMCs were similar to that of Pt/C in the low overvoltage region (Figure 4b). Furthermore, NPOMC-L1 showed exchange current density of 6.40×10^{-6} mA cm^{-2}, which was 76.8% that of Pt/C (Figure 4c).

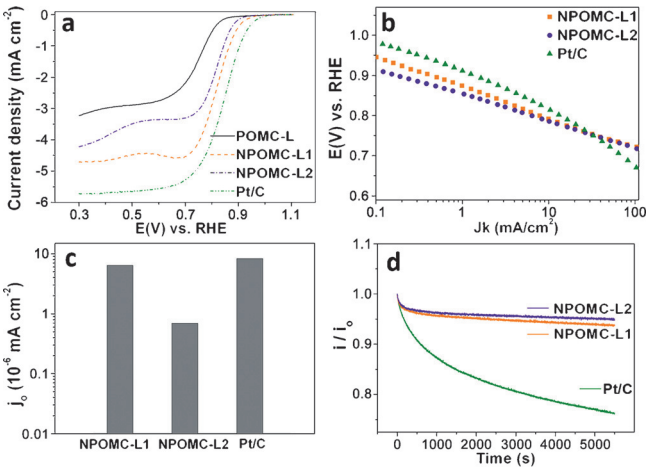

Figure 4. a) LSV polarization curves, b) corresponding Tafel plots, and c) exchange current density of the catalysts. d) Current–time (*i-t*) chronoamperometric response of the catalysts at 0.4 V.

The LSV with RDE measurement at various rotation speeds was conducted to evaluate the electron transfer number in ORR using the Koutecky–Levich (K-L) equation (Figure S10). The electron transfer number at 0.75 V was calculated to be 3.7 in NPOMC-L1, which is higher than that of NPOMC-L2 (3.5) and POMC-L (3.1), and approaches that of Pt/C (3.9). Cyclic voltammetry (CV) tests in an electrolyte containing 1M methanol were performed to assess the tolerance of both NPOMCs to methanol. Selective oxygen reduction is quite important in cathode catalysts because small molecule fuels such as methanol, which are injected in the anode, may cross through the polymer membrane to the cathode. No peak related to methanol oxidation was observed, and thus selective ORR occurred in both NPOMC-Ls (Figure S11). To test the durability of the catalyst, the decrease of current density was measured using chronoamperometry at 0.4 V with a rotation speed of 1600 rpm. Over a period of 5500 s, Pt/C lost 23.7% of its initial current density, whereas NPOMC-L1 lost only 6.2% and NPOMC-L2 lost only 5.2% (Figures 4d and S12). The better durability of NPOMCs would be originated from strong covalent binding of heteroatoms to carbon.[2d,e]

Single-cell tests were conducted to quantify the performance improvement achieved by the additional nitrogen doping and investigate the effect of doping site position (Figure 5a). Interestingly, the results obtained in the single-cell test were totally different from those in the half-cell test (Figure 5b). The cell performance of MEA based on NPOMC-L1 was not improved compared with that of POMC-L, although NPOMC-L1 exhibited the best activity in the half-cell test. In contrast, NPOMC-L2-based MEA

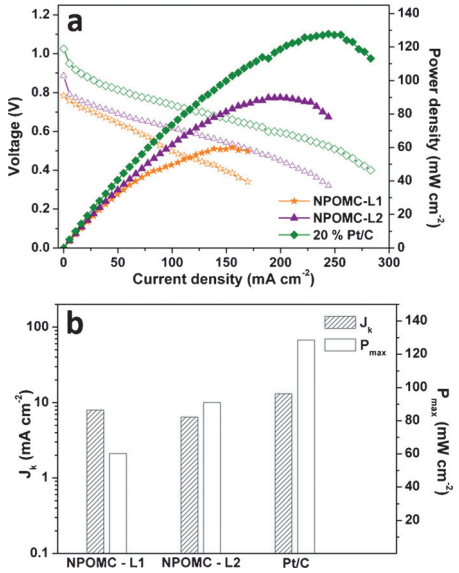

Figure 5. a) Polarization curves of MEAs at 60°C; open and closed symbols correspond to cell voltage and power density, respectively. b) Comparison of kinetic current density at 0.8 V in the half-cell test and maximum power density in the single-cell test.

exhibited a remarkable on-set potential in the single-cell test. The maximum power density of NPOMC-L2 was 1.4 times higher than that of POMC-L; furthermore, it was 70% that of Pt/C, which is a significant achievement considering the previous results.[2d,3b] Because the catalytic activity for ORR is higher in NPOMC-L1 than in NPOMC-L2, the outstanding single-cell performance of NPOMC-L2 probably occurs because its higher accessibility to nitrogen doping sites causes an enhancement of mass transport and better utilization of doping sites in the catalyst layer. The difference in the cell performance between NPOMC-L2 and NPOMC-L3 further supports the relationship between the doping site position and the single cell performance. NPOMC-L3 exhibited much lower maximum power density than NPOMC-L2 because a large fraction of nitrogen doping sites of NPOMC-L3 would be located in the microporous region (Figures S6, S13, and S14).

In this work, the trend observed in half-cell tests is not directly transferable to the trend observed in single-cell tests, which should always be considered for catalyst design. Because the MEAs based on metal-free catalysts require a relatively thick catalyst layer, the influence of mass transport in the catalyst layer is more critical than in Pt/C-based MEAs. Therefore, both half-cell and single-cell data must be considered when designing high-performance nanostructured catalysts, although many previous reports on high-performance heteroatom-doped carbon catalysts have considered only half-cell results.[2b,c,e,3a,c,5a,b]

We have demonstrated the effect of the pore size and doping site position on the single-cell performance of metal-free catalysts using well-defined ordered mesoporous carbon systems. The single-cell tests prove that control of pore size and doping-site position directly affects the cell performance by changing the mass-transport properties and utilizing the doping sites in the catalyst layer. NPOMC with precisely controlled doping sites to be near the large mesopores exhibited a remarkable on-set potential and achieved 70% of the maximum power density of Pt/C. It is expected that the effective doping strategy developed in this work may be widely applicable to various electrochemical catalytic systems in addition to fuel cells.

Keywords: electrocatalysis · fuel cells · mesoporous materials · metal-free catalysts · oxygen reduction reaction

How to cite: *Angew. Chem. Int. Ed.* **2015**, *54*, 9230–9234
Angew. Chem. **2015**, *127*, 9362–9366

[1] J. R. Varcoe, R. C. T. Slade, *Fuel Cells* **2005**, *5*, 187.
[2] a) Y. Jiao, Y. Zheng, M. Jaroniec, S. Z. Qiao, *J. Am. Chem. Soc.* **2014**, *136*, 4394; b) K. P. Gong, F. Du, Z. H. Xia, M. Durstock, L. M. Dai, *Science* **2009**, *323*, 760; c) W. J. Jiang, J. S. Hu, X. Zhang, Y. Jiang, B. B. Yu, Z. D. Wei, L. J. Wan, *J. Mater. Chem. A* **2014**, *2*, 10154; d) T. Palaniselvam, M. O. Valappil, R. Illathvalappil, S. Kurungot, *Energy Environ. Sci.* **2014**, *7*, 1059; e) Z. W. Liu, F. Peng, H. J. Wang, H. Yu, W. X. Zheng, J. A. Yang, *Angew. Chem. Int. Ed.* **2011**, *50*, 3257; *Angew. Chem.* **2011**, *123*, 3315; f) W. Ding, Z. D. Wei, S. G. Chen, X. Q. Qi, T. Yang, J. S. Hu, D. Wang, L. J. Wan, S. F. Alvi, L. Li, *Angew. Chem. Int. Ed.* **2013**, *52*, 11755; *Angew. Chem.* **2013**, *125*, 11971.
[3] a) H. L. Jiang, Y. H. Zhu, Q. Feng, Y. H. Su, X. L. Yang, C. Z. Li, *Chem. Eur. J.* **2014**, *20*, 3106; b) Y. J. Sa, C. Park, H. Y. Jeong, S. H. Park, Z. Lee, K. T. Kim, G. G. Park, S. H. Joo, *Angew. Chem. Int. Ed.* **2014**, *53*, 4102; *Angew. Chem.* **2014**, *126*, 4186; c) X. F. Liu, M. Antonietti, *Adv. Mater.* **2013**, *25*, 6284.
[4] a) O. H. Kim, Y. H. Cho, S. H. Kang, H. Y. Park, M. Kim, J. W. Lim, D. Y. Chung, M. J. Lee, H. Choe, Y. E. Sung, *Nat. Commun.* **2013**, *4*, 2473; b) M. C. Orilall, U. Wiesner, *Chem. Soc. Rev.* **2011**, *40*, 520.
[5] a) J. Liang, X. Du, C. Gibson, X. W. Du, S. Z. Qiao, *Adv. Mater.* **2013**, *25*, 6226; b) D. S. Yang, D. Bhattacharjya, S. Inamdar, J. Park, J. S. Yu, *J. Am. Chem. Soc.* **2012**, *134*, 16127; c) R. L. Liu, D. Q. Wu, X. L. Feng, K. Mullen, *Angew. Chem. Int. Ed.* **2010**, *49*, 2565; *Angew. Chem.* **2010**, *122*, 2619; d) J. Liang, Y. Zheng, J. Chen, J. Liu, D. Hulicova-Jurcakova, M. Jaroniec, S. Z. Qiao, *Angew. Chem. Int. Ed.* **2012**, *51*, 3892; *Angew. Chem.* **2012**, *124*, 3958.
[6] W. Xiao, D. L. Wang, X. W. Lou, *J. Phys. Chem. C* **2010**, *114*, 1694.
[7] K. Egeblad, C. H. Christensen, M. Kustova, C. H. Christensen, *Chem. Mater.* **2008**, *20*, 946.
[8] J. C. Groen, W. D. Zhu, S. Brouwer, S. J. Huynink, F. Kapteijn, J. A. Moulijn, J. Perez-Ramirez, *J. Am. Chem. Soc.* **2007**, *129*, 355.
[9] a) J. Hwang, C. Jo, K. Hur, J. Lim, S. Kim, J. Lee, *J. Am. Chem. Soc.* **2014**, *136*, 16066; b) J. Hwang, S. H. Woo, J. Shim, C. Jo, K. T. Lee, J. Lee, *ACS Nano* **2013**, *7*, 1036; c) M. C. Orilall, F. Matsumoto, Q. Zhou, H. Sai, H. D. Abruna, F. J. DiSalvo, U. Wiesner, *J. Am. Chem. Soc.* **2009**, *131*, 9389.
[10] W. C. Sheng, S. Chen, E. Vescovo, Y. Shao-Horn, *J. Electrochem. Soc.* **2012**, *159*, B96.

Received: February 18, 2015
Revised: April 24, 2015
Published online: June 18, 2015

